Exploring the Role of the Solvent in the Denaturation of a Protein: A Molecular Dynamics Study of the DNA Binding Domain of the 434 Repressor†

Celia A. Schiffer,‡,§ Volker Dötsch,‖,⊥ Kurt Wüthrich,‖ and Wilfred F. van Gunsteren*,‡

Laboratorium für Physikalische Chemie, ETH-Zentrum, 8092 Zürich, Switzerland, and Institut für Molekularbiologie und Biophysik, ETH-Hönggerberg, 8093 Zürich, Switzerland

Received May 23, 1995; Revised Manuscript Received August 28, 1995⊗

ABSTRACT: Molecular dynamics simulations of the DNA binding domain of 434 repressor are presented which aim at unraveling the role of solvent in protein denaturation. Four altered solvent models, each mimicking various possible aspects of the addition of a denaturant to the aqueous solvent, were used in the simulations to analyze their effects on the stability of the protein. The solvent was altered by selectively changing the Coulombic interaction between water and protein atoms and between different water molecules. The use of a modified solvent model has the advantage of mimicking the presence of denaturant without having denaturant molecules present in the simulation, which would require much longer simulations. In these simulations, only an increase in the solvent−protein Coulombic interaction causes initiation of protein unfolding in a manner consistent with NMR data. The altered solvent thus provides a model of a denaturing environment for studying protein unfolding.

When protein unfolding is induced by the addition of a denaturant such as urea in an aqueous environment, the exact interactions at the atomic level that are responsible for the unfolding are not known. The denaturant may physically diffuse into the protein and interact directly with protein atoms, thereby disrupting intramolecular hydrogen bonds and van der Waals contacts (Lapanje et al., 1976; Pace, 1986; Pace et al., 1992). These are the interactions that stabilize the tertiary and secondary structure of the molecule, and thus their disruption may cause the protein to unfold. Or, the denaturant could induce protein unfolding indirectly by disrupting the solvent environment. In this case several mechanisms are possible. The denaturant might disrupt the water−water interactions, which would make the interaction between water and protein relatively more favorable. The water molecules might then penetrate into the protein, disrupt internal hydrogen bonds, and cause the protein to unfold. Alternatively, the denaturant might bind strongly to water molecules, which would make the relative interactions between the protein and water less favorable. Experimentally, determining which effect or combination of effects is causing the denaturation is very difficult. Recent NMR studies have shown both, selective binding of urea molecules in surface grooves of folded proteins (Liepinsh & Otting, 1994) and preferential interactions between individual urea molecules and side-chain methyl groups of an unfolded protein (Dötsch et al., 1995a). However, whether these latter interactions are the cause or a consequence of the unfolding of the molecule has not been determined. Computational work has shown the likelihood of direct interactions between urea molecules and aromatic hydrocarbons (Duffy et al., 1993). Protein denaturation can be induced not only by the addition of denaturants such as urea, guanidinium hydrochloride, or NaSCN but also by other methods such as lowering or raising the temperature or increasing the pressure. Whether protein denaturation proceeds by one or several different mechanisms induced by the different denaturing conditions is unclear.

In contrast to experimental techniques, molecular dynamics (MD) simulation offers the possibility to monitor the interactions of the protein with its environment directly by examining each structure along the trajectory and recording how it changes with time. The major limitation of present MD simulations is, however, the short time scale, on the order of nanoseconds. Within this time scale simulating a protein at equilibrium with an aqueous mixture of ions and denaturants is not practical. A simulation of such a mixture takes nanoseconds to equilibrate and sample the spatial distribution of the molecules properly. In shorter simulations, salt molecules would not have sufficient time to diffuse and equilibrate around a protein. A way around this limitation is to simulate a homogeneous aqueous environment and mimic the effect of denaturants on the protein by changing the water−water or the water−protein interaction. By changing these interactions of the water and monitoring what happens to the structure of the protein, one may determine the interactions that are most critical for keeping the protein structurally intact.

434 is a lysogenic bacteriophage which activates its own transcription by its Cro and repressor proteins. The 434 repressor binds to DNA at the two operator regions, OR1 and OR2, turns off the synthesis of Cro, and activates its own transcription. The three-dimensional structure of a 69-residue DNA binding domain of 434 repressor, 434(1−69), has been determined crystallographically both as the free monomeric protein (Mondragon et al., 1989) and twice as a protein dimer bound to synthetic DNA duplex sequences

† Financial support by the Kommission zur Förderung der wissenschaftlichen Forschung (project 2223.1) is gratefully acknowledged.

‡ ETH-Zentrum.

§ Present address: Department of Protein Engineering, Genentech, Inc., 460 Point San Bruno Blvd., S. San Francisco, CA 94080.

‖ ETH-Hönggerberg.

⊥ Present address: Department of Biological Chemistry and Molecular Pharmacology, Harvard Medical School, 240 Longwood Ave., Boston, MA 02115.

⊗ Abstract published in *Advance ACS Abstracts,* October 15, 1995.

0006-2960/95/0434-15057$09.00/0

which correspond to each of its operator sites (Shimon & Harrison, 1993). The structure of free 434(1−69) has also been determined by NMR spectroscopy (Neri et al., 1992a). The 434(1−69) structure belongs to the helix−turn−helix DNA binding proteins and is not stabilized by any disulfide bonds or metal ions.

The N-terminal DNA binding domain 434(1−69) was obtained by expression of the intact repressor protein in *Escherichia coli* followed by proteolytic cleavage (Mondragon et al., 1989). In both the crystal and solution structures of 434(1−69) the C-terminal hexapeptide is disordered (Mondragon et al., 1989; Neri et al., 1992a). For further experimental denaturation studies the polypeptide segment 434(1−63) was therefore cloned and expressed in *E. coli* (Neri et al., 1992c). It was then discovered that at pH 7.6 and temperatures around 290 K a solution of 434-(1−63) in 7 M urea contains a small percentage of a folded conformation (Dötsch et al., 1995b). Further experiments showed that the percentage of folded conformation can be increased by adding certain salts or nonionic compounds. These results invite further study of the role of urea and water molecules in the denaturation process (Dötsch et al., 1995b) and led to the molecular dynamics simulations presented here as well as to further structure determinations under denaturing solution conditions (K. Pervushin, O. Schott, G. Siegal, M. Billeter, and K. Wüthrich, personal communication). The native structure and its thermal stability, with a melting temperature near 70 °C in an aqueous environment at neutral pH, are nearly identical for 434(1−69) and 434(1−63). Since by both structure determination techniques only the first 63 residues were found to be ordered in 434(1−69) and since this is in concert with ongoing experimental studies of 434-(1−63), the simulations were performed for the polypeptide 434(1−63). With regard to the results of the MD simulations it is of special interest that in 7 M urea a structured hydrophobic cluster is formed by the octapeptide segment of residues 53−60 of both 434(1−63) and 434(1−69), as well as 434(44−63) (Neri et al., 1992b,d). This hydrophobic cluster is related to the native structure formed by residues 53−60 in the folded protein by strictly local structural rearrangements involving three amino acid side chains (Neri et al., 1992b).

In this paper we report a series of six MD simulations (ranging in time from 250 to 500 ps) in an explicit aqueous environment, in which the structure of the free 434(1−63) monomer was used as the starting point. The interaction function of the solvent was modified in a variety of ways so as to assess which interactions are most critical in maintaining the native fold of the molecule. Since there is some nonrandom structure seen experimentally by NMR under strongly denaturing conditions, this system might also enable an assessment of whether the conclusions drawn from the simulations are consistent with experimental observations.

Previous computer simulations of protein denaturation have used high temperatures to speed up the unfolding process (Caflisch & Karplus, 1994; Daggett & Levitt, 1992, 1993; Mark & van Gunsteren, 1992; Tirado-Rives & Jorgensen, 1993), introduced artificial centrifugal driving forces (Hao et al., 1993), or used increased pressure (Hünenberger et al., 1995). Recent work has used the technique of parallel MD simulations to investigate the relative structural stability of a protein, once disulfide bonds have been removed (Schiffer and van Gunsteren, 1995). The current study investigates how changes in the solvent affect the structural stability of the protein.

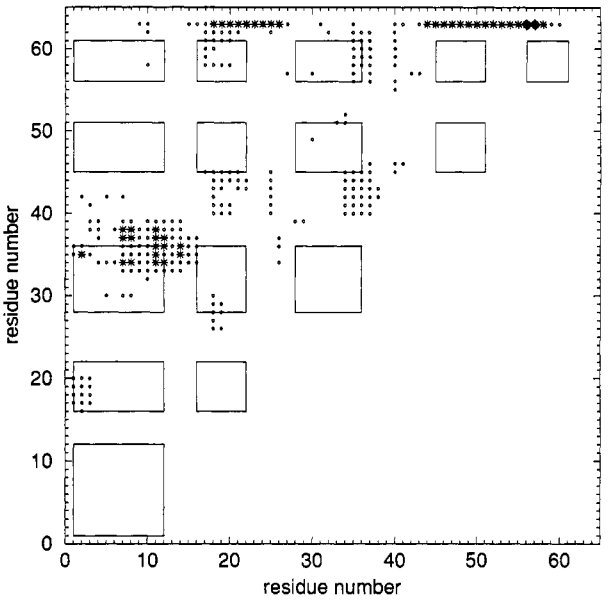

FIGURE 1: Distance difference map between the crystal structure of 434(1−63) and the structure after 380 ps of molecular dynamics simulation of the standard system with normal SPC/E water at 300 K. A diamond shows a deviation of more than 3 Å, a star a deviation of more than 2 Å, and a dot a deviation of more than 1 Å.

METHODS

All the molecular dynamics simulations were performed with the GROMOS simulation package (van Gunsteren & Berendsen, 1987) and 37C4 united atom force field. The SPC/E water model (Berendsen et al., 1987) was used. For the interaction between a neutral carbon and SPC/E water oxygen a modified value of C12 = 793.3 (kcal mol^{-1} Å^{12})$^{1/2}$ was used (Mark et al., 1994).

The ordered region, residues 1−63 (613 atoms), in the crystal structure of the free 434(1−69) was used as the initial and reference structure for the simulations. The protein was placed in a box of equilibrated water, and all water molecules for which the oxygen atom was closer than 2.39 Å to any non-hydrogen protein atom were removed. The system was a periodic truncated octahedron with a 9.0 Å minimum distance between the protein and the edge of the box. The initial velocities were taken from a Maxwellian distribution at 50 K. Covalent bond lengths were constrained using the SHAKE procedure (Ryckaert et al., 1977) with relative tolerance of 10^{-4}. The time step used in the leap-frog integration scheme was 0.002 ps. A cutoff radius of 8.0 Å for the nonbonded interactions was used in conjunction with a pair list which was updated every 10 time steps. In each simulation the temperature of the system was maintained by weak coupling to a heat bath (Berendsen et al., 1984) with a coupling constant of 0.1 ps. The simulations were performed at constant pressure using weak coupling to a pressure bath (Berendsen et al., 1984) with a coupling constant of 0.1 ps.

The standard protein−water system contained one protein molecule and 2031 water molecules and was equilibrated by harmonically restraining (force constant 1000 kJ mol^{-1} Å^{-2}) the protein atoms to their crystallographic positions.

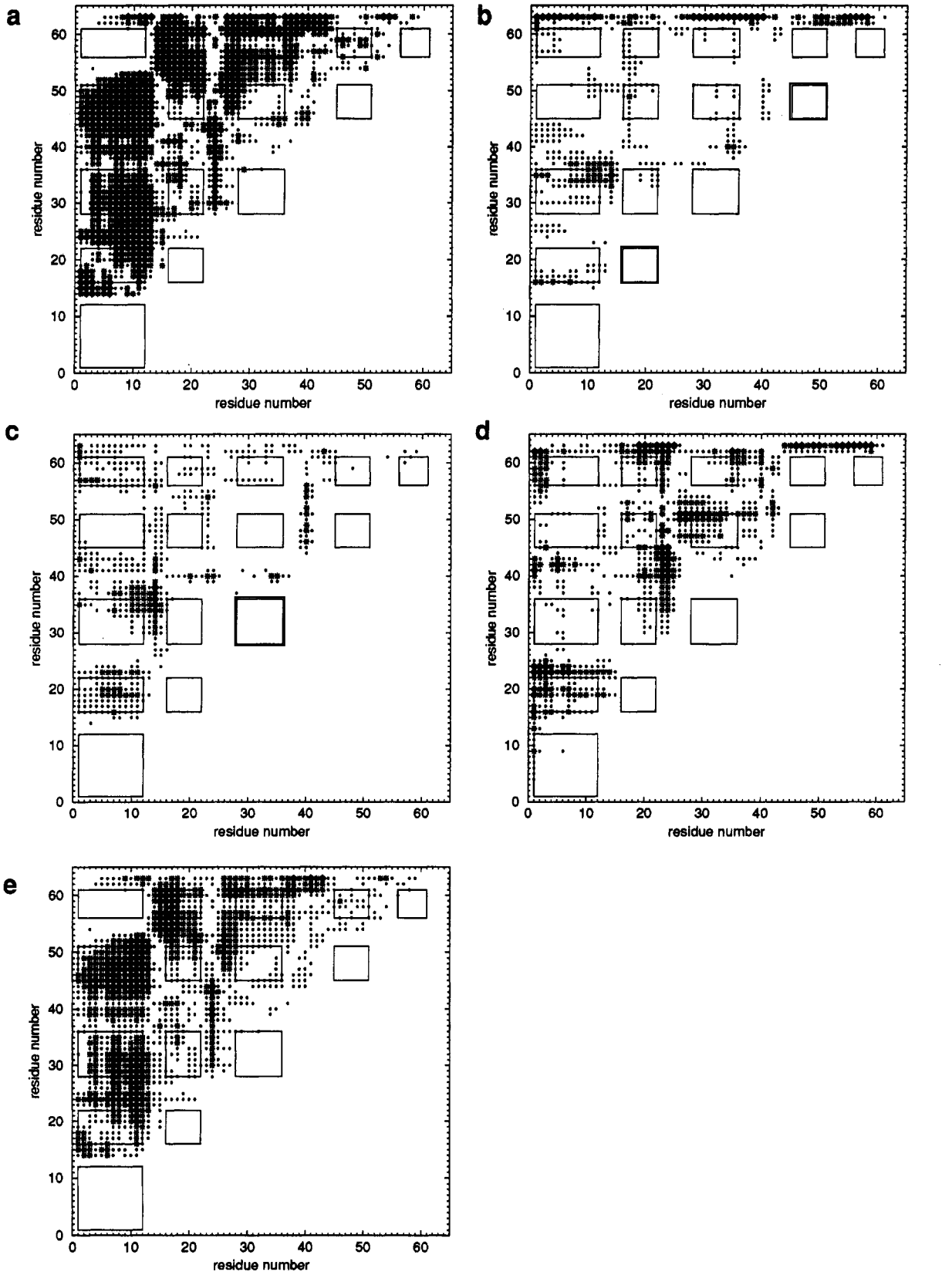

FIGURE 2: Distance difference maps between the crystal structure of 434(1−63) and the structures after 250 ps of molecular dynamics under the four altered solvent conditions using the same scale as in Figure 1. Panels: (a) SPM, solvent−protein more interaction; (b) SPL, solvent−protein less interaction; (c) SSM, solvent−solvent more interaction; (d) SSL, solvent−solvent less interaction; (e) SPM [as in (a)] with a coarser scale, where a diamond shows a deviation of more than 5 Å, a star a deviation of more than 3 Å, and a dot a deviation of more than 1 Å.

Energy minimization was performed to remove unfavorable nonbonded interactions. Over a period of 60 ps the temperature was slowly increased from 50 to 300 K, and then the harmonic restraints were released. The system was simulated at 300 K at a constant pressure of 1 atm for another 380 ps. The resulting equilibrated structure of the standard

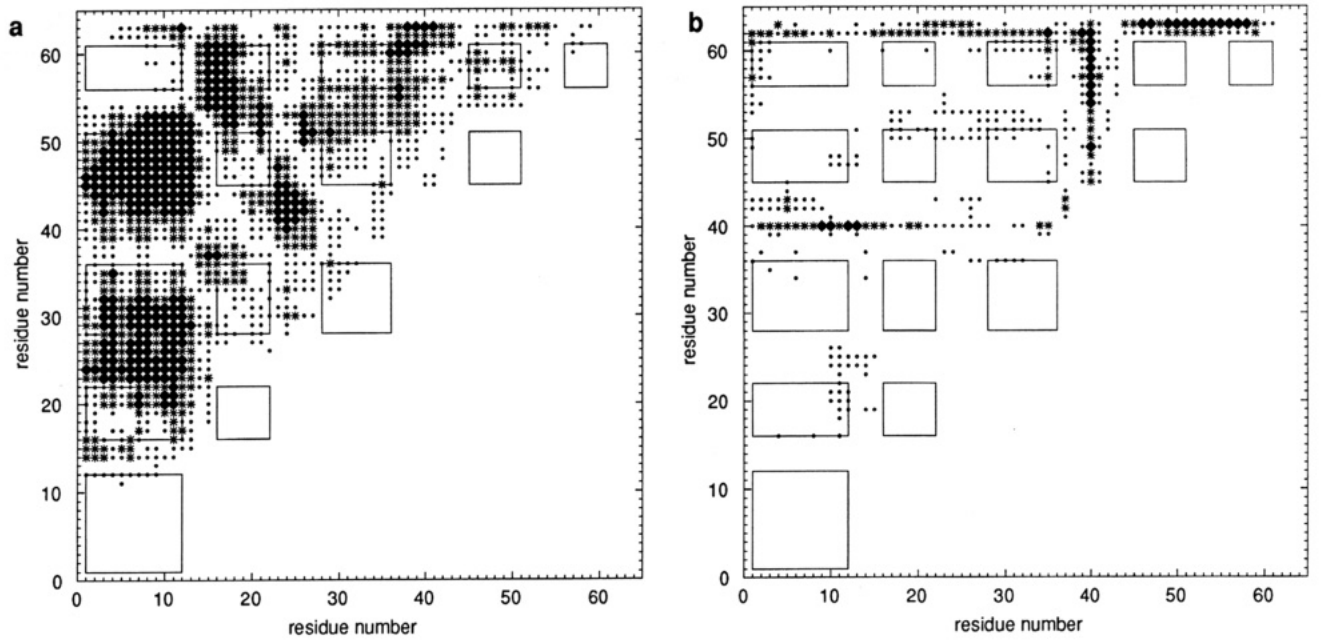

FIGURE 3: Distance difference maps between the crystal structure of 434(1−63) and the structures after (a) 500 ps under the SPM solvent condition (using the same scale as in Figure 2e) and (b) 350 ps under the SSL solvent condition (using the same scale as in Figure 1).

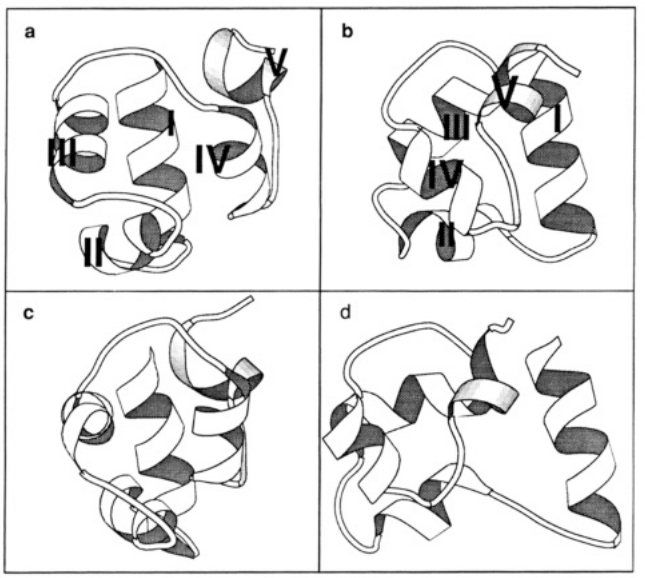

FIGURE 4: Molscript (Kraulis, 1991) diagram of the crystal structure of the DNA binding domain of residues 1−63 of the 434 repressor (a). The region which is shaded forms a nonrandom hydrophobic cluster in 7 M urea. An orthogonal view is presented in (b). The resulting structure after 500 ps of molecular dynamics under SPM solvent conditions: the orientation in panel c corresponds to that of panel a, and that in panel d corresponds to that of panel b.

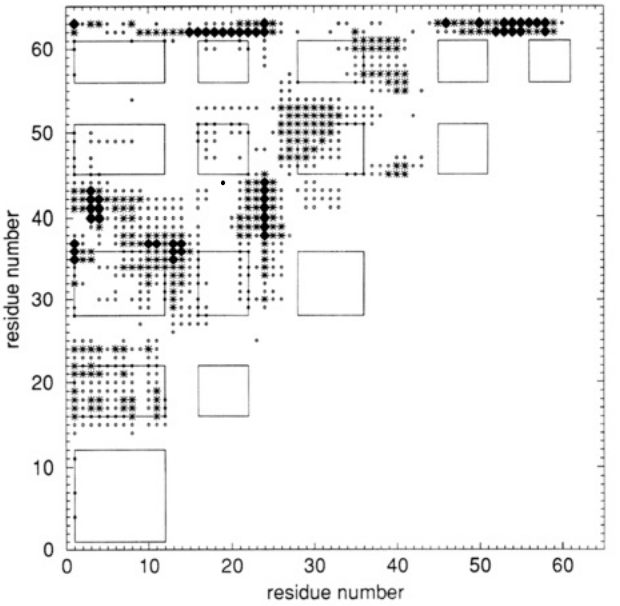

FIGURE 5: Distance difference map between the crystal structure of 434(1−63) and the structure after 500 ps of molecular dynamics at an elevated temperature of 360 K using the standard system with SPC/E water (same scale as in Figure 1).

protein−water system was used to branch off the subsequent simulations with modified interactions.

To mimic various solvent environments, the interaction function of the SPC/E water molecules was changed in four ways. In each model only the nonbonded Coulombic interactions were altered. In the first model, SPM (solvent−protein more interaction), the water−protein Coulombic interaction was scaled to 110% of its original value. In the second model, SPL (solvent−protein less interaction), the water−protein Coulombic interaction was scaled to 90% of its original value. In the third model, SSM (solvent−solvent more interaction), the water−water Coulombic interaction was scaled to 110% of its original value. In the fourth model, SSL (solvent−solvent less interaction), the water−water Coulombic interaction was scaled to 90% of its original value. The degree of perturbation of the solvent interactions, 10% more or less, was chosen so as to obtain a small perturbation, for which the onset of denaturation may be observed within a few hundred picoseconds. By applying the same size of perturbation in the various models and performing simulations of equal length, starting from the same structure, it was possible to analyze the relative destabilizing effects of each of these models.

The simulations using the SPM and the SPL solvent models started from the equilibrated standard system along with the corresponding velocities at 300 K. The protein was simulated under SPL solvent conditions for 250 ps and under SPM solvent conditions for a total of 500 ps, both at 300 K and 1 atm.

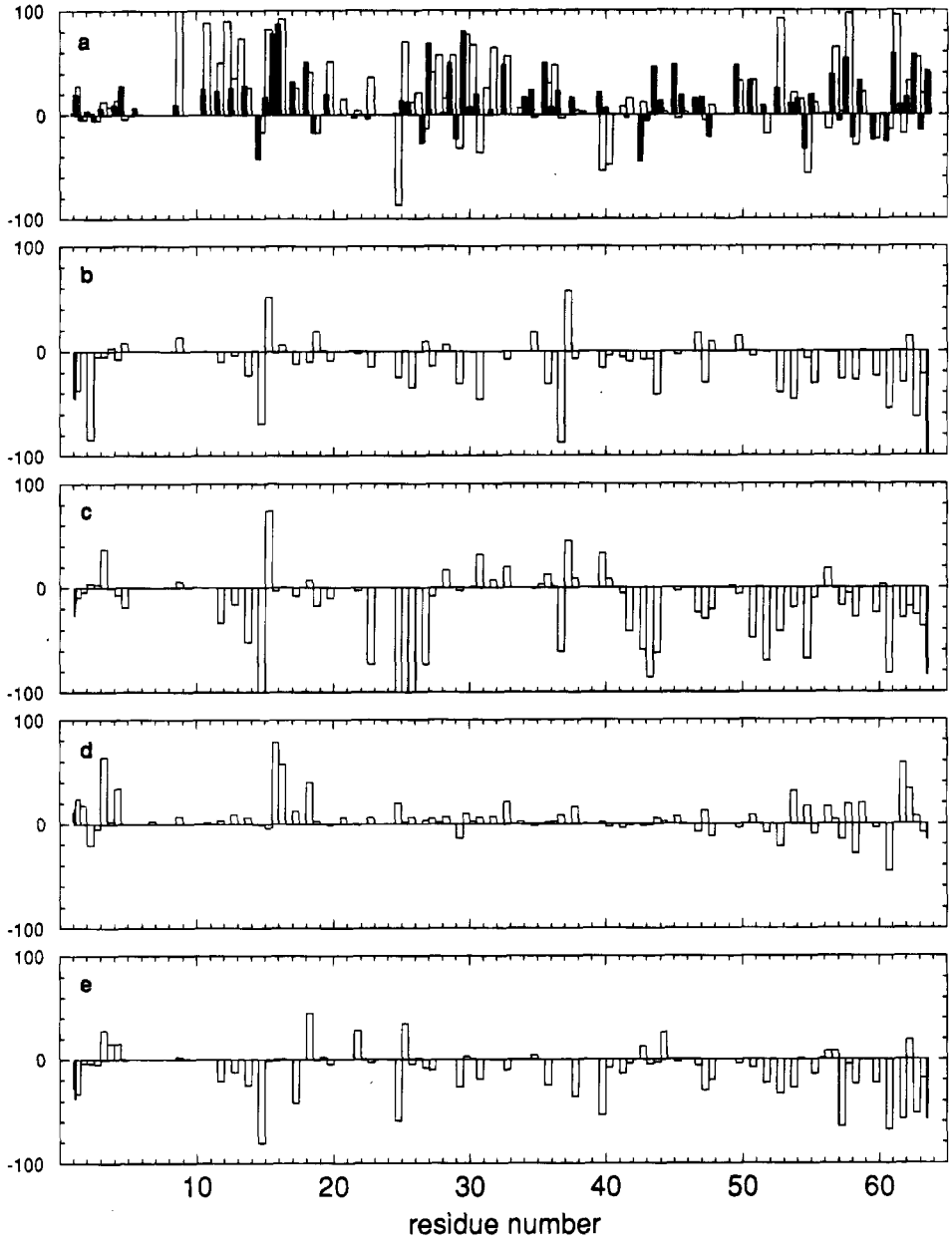

FIGURE 6: Differences in hydrogen bonding between polar backbone atoms and water in the simulations with altered solvent interactions with respect to the simulation using the standard system with the normal water interactions: Panels: (a) SPM, solid bars 150−250 ps, open bars 400−500 ps; (b) SPL, 150−250 ps; (c) SSM, 150−250 ps; (d) SSL, 150−250 ps; (e) standard system at 360 K, 400−500 ps. The degree of hydrogen bonding is measured as a percentage over a period of 100 ps simulation.

For the simulations of the protein in the SSM and SSL solvent conditions, the standard equilibrium protein configuration was first stripped of the equilibrated water molecules and then immersed in a bath of water which had been equilibrated with the altered water−water interaction. The number of water molecules in the SSM system was 2208, and in the SSL system it was 2080. As in the equilibration of the standard system, strong harmonic restraints (force constant 1000 kJ mol^{-1} $Å^{-2}$) were applied to the protein atoms while the system was brought slowly from 50 to 300 K, and the harmonic restraints were released over 50 ps. The ensuing simulations were performed for a total of 250 ps for the SSM solvent environment and 350 ps for the SSL solvent environment, both at 300 K and 1 atm.

For comparison, an additional simulation with the standard protein−water system was performed to assess the stability of the molecule with respect to an increase in temperature. This technique has been previously used as a method to computationally denature a molecule. The measured melting temperatures of 431(1−69) (Neri et al., 1992a) and 434(1−63) (unpublished results) are quite high at approximately 350 K. Our simulation was performed at 360 K and 1 atm, only slightly higher than the melting point, and thus remains in the physically reasonable temperature range. This simulation was run for a total of 500 ps.

For each simulation the hydrogen-bonding interactions were examined for the last 100 ps of each trajectory. Hydrogen bonds between the solvent and both the backbone and side chains of the protein, as well as the intramolecular hydrogen bonds of the protein, were examined as a function of time. A hydrogen bond was defined by a distance between the hydrogen and the acceptor atom of less than 2.5 Å and a donor−hydrogen−acceptor angle of greater than 135°.

Table 1: Percentage of Hydrogen Bonding of Side-Chain Atoms to Water over a 100 ps Time Period[a]

residue no.	residue	atom				change rel to standard simulation					
		D	H	A	standard	SPM	SPM500	SPL	SSL	SSM	heat
1	Ser	OG	HG	OW	97	1	1	−8	−15	0	−6
1	Ser	OW	HW1	OG	9	−4	−1	1	5	7	−3
3	Ser	OG	HG	OW	97	1	1	−20	−0	−2	−42
3	Ser	OW	HW2	OG	46	29	38	13	19	2	−4
4	Ser	OG	HG	OW	95	4	2	−95	1	1	−3
4	Ser	OW	HW1	OG	4	26	1	−3	39	−1	18
5	Arg	NE	HE	OW	88	3	5	−83	−13	−10	−43
5	Arg	NH1	HH11	OW	54	8	−14	13	10	−34	11
5	Arg	NH1	HH12	OW	4	−4	−4	−4	4	3	−4
5	Arg	NH2	HH22	OW	62	6	−30	−58	3	−39	2
5	Arg	NH2	HH21	OW	54	17	16	−6	10	12	−31
7	Lys	NZ	HZ1	OW	78	8	8	−16	8	−6	−12
7	Lys	NZ	HZ2	OW	69	20	13	−38	16	−41	−11
7	Lys	NZ	HZ3	OW	73	11	13	−54	5	−36	−30
8	Ser	OG	HG	OW	92	7	8	−17	−27	4	0
8	Ser	OW	HW1	OG	77	−31	−8	−61	−48	−9	−2
9	Lys	NZ	HZ2	OW	75	14	15	−4	17	−17	7
9	Lys	NZ	HZ3	OW	81	4	11	−57	4	−11	−6
9	Lys	NZ	HZ1	OW	90	−6	−2	−72	−5	−40	−52
10	Arg	NE	HE	OW	27	64	66	−27	64	19	−17
10	Arg	NH1	HH11	OW	82	−5	−11	−7	−11	−13	−22
10	Arg	NH1	HH12	OW	0	70	19	0	89	0	16
10	Arg	NH2	HH22	OW	54	19	16	11	29	10	1
10	Arg	NH2	HH21	OW	67	8	4	−64	−28	−48	−47
12	Gln	NE2	HE22	OW	85	1	−11	−20	−13	−22	−23
12	Gln	NE2	HE21	OW	68	16	13	−1	19	8	10
12	Gln	OW	HW2	OE1	98	49	51	−71	18	−14	−32
16	Asn	ND2	HD22	OW	89	−3	−2	−24	−76	−5	−41
16	Asn	ND2	HD21	OW	90	3	−5	−15	0	−1	−26
16	Asn	OW	HW1	OD1	60	1	−12	−11	−8	−47	5
17	Gln	NE2	HE21	OW	0	3	0	0	45	7	52
17	Gln	NE2	HE22	OW	1	29	−1	−1	85	−1	7
17	Gln	OW	HW2	OE1	5	92	85	0	74	46	14
19	Glu	OW	HW2	OE1	289	70	73	−161	27	−63	−82
19	Glu	OW	HW1	OE2	262	96	97	−53	54	−59	−63
22	Gln	NE2	HE22	OW	88	−3	−31	−27	−17	−20	−21
22	Gln	NE2	HE21	OW	70	19	16	−14	10	8	−4
22	Gln	OW	HW1	OE1	127	34	25	−45	−4	10	−26
23	Lys	NZ	HZ2	OW	89	1	1	−36	−14	−19	−10
23	Lys	NZ	HZ3	OW	85	−1	2	−12	−1	−11	−8
23	Lys	NZ	HZ1	OW	83	3	4	−51	1	−29	−1
26	Thr	OG1	HG1	OW	95	−28	−95	−5	−11	−4	−9
26	Thr	OW	HW1	OG1	58	8	35	−56	−33	−56	−37
27	Thr	OG1	HG1	OW	97	3	−1	−1	0	−14	−2
27	Thr	OW	HW2	OG1	42	34	27	−37	−6	−29	−9
28	Gln	NE2	HE22	OW	4	78	85	42	36	33	−4
28	Gln	NE2	HE21	OW	0	70	8	3	67	59	47
28	Gln	OW	HW1	OE1	134	25	−85	−24	3	−21	−62
29	Gln	NE2	HE21	OW	78	6	8	−15	−2	4	−48
29	Gln	NE2	HE22	OW	66	7	16	−2	−25	−64	−51
29	Gln	OW	HW2	OE1	124	22	22	−31	18	6	−2
30	Ser	OG	HG	OW	70	30	11	−66	−5	−57	−30
30	Ser	OW	HW1	OG	78	29	−1	5	13	−74	−31
32	Glu	OW	HW1	OE1	319	55	43	−40	17	−42	−74
32	Glu	OW	HW1	OE2	195	191	166	−48	115	−7	30
33	Gln	NE2	HE21	OW	63	16	5	8	10	8	3
33	Gln	NE2	HE22	OW	62	25	29	−55	20	12	−33
33	Gln	OW	HW2	OE1	121	12	−4	−20	−11	−24	−17
35	Glu	OW	HW2	OE1	281	87	100	−78	48	−95	−116
35	Glu	OW	HW1	OE2	242	110	137	−185	37	−82	−41
36	Asn	ND2	HD21	OW	82	3	−6	−8	−4	−4	−26
36	Asn	ND2	HD22	OW	69	20	15	−3	13	14	−30
36	Asn	OW	HW1	OD1	90	23	47	−42	15	−51	−5
38	Lys	NZ	HZ2	OW	81	7	7	−4	4	1	2
38	Lys	NZ	HZ1	OW	85	−4	3	−37	−5	−9	−3
38	Lys	NZ	HZ3	OW	85	1	3	−54	−2	−29	−7
39	Thr	OG1	HG1	OW	89	10	6	−83	−8	−40	−24
39	Thr	OW	HW2	OG1	50	−21	39	−40	−0	−14	3
40	Lys	NZ	HZ1	OW	83	3	6	−5	1	−2	−9
40	Lys	NZ	HZ2	OW	85	3	3	−4	−4	−5	−15
40	Lys	NZ	HZ3	OW	84	1	3	−7	−7	−3	−19
41	Arg	NE	HE	OW	85	6	−4	3	4	−12	−19
41	Arg	NH1	HH11	OW	75	3	4	−12	−14	9	−12

Table 1 (Continued)

residue no.	residue	atom D	atom H	atom A	standard	change rel to standard simulation SPM	SPM500	SPL	SSL	SSM	heat
41	Arg	NH1	HH12	OW	67	−0	7	−14	8	18	−3
41	Arg	NH2	HH21	OW	76	−3	−9	−16	2	13	−11
41	Arg	NH2	HH22	OW	72	3	5	−3	−8	9	−16
43	Arg	NE	HE	OW	84	−1	3	−3	−5	−13	−4
43	Arg	NH1	HH11	OW	65	4	10	−52	−6	−21	−8
43	Arg	NH1	HH12	OW	49	19	17	8	18	18	5
43	Arg	NH2	HH22	OW	60	5	9	−55	8	5	1
43	Arg	NH2	HH21	OW	68	3	5	−12	−9	−31	−8
47	Glu	OW	HW1	OE1	327	22	30	−118	−28	−196	−100
47	Glu	OW	HW1	OE2	322	40	49	−227	21	−220	−77
50	Ser	OG	HG	OW	97	2	2	−4	1	0	−7
50	Ser	OW	HW1	OG	85	32	25	−46	19	13	1
55	Ser	OG	HG	OW	95	2	4	−1	0	4	−3
55	Ser	OW	HW2	OG	41	26	4	−31	−16	−29	−4
57	Asp	OW	HW2	OD1	288	66	67	−60	54	−9	−2
57	Asp	OW	HW1	OD2	295	77	82	−8	55	−55	−10
58	Trp	NE1	HE1	OW	60	6	9	−8	−4	−0	−7
61	Asn	ND2	HD21	OW	56	31	36	−5	6	−9	−1
61	Asn	ND2	HD22	OW	9	78	88	−9	51	−9	37
61	Asn	OW	HW2	OD1	117	3	17	−19	8	−31	−12
63	Thr	OG1	HG1	OW	90	−13	5	−5	−19	2	−35
63	Thr	OW	HW1	OG1	114	−39	1	−108	−9	−31	−22

[a] D, H, and A are the donating, hydrogen, and accepting atoms in the hydrogen bond; standard refers to the standard system with normal SPC/E water, 340−440 ps. Abbreviations: SPM, solvent−protein more interaction, 150−250 ps; SPM500, same from 400 to 500 ps; SPL, solvent−protein less interaction, 150−250 ps; SSM solvent−solvent more interaction, 150−250 ps; SSL, solvent−solvent less interaction, 150−250 ps; heat, SCP/E water at 360 K, 150−250 ps.

The backbone conformations of the final structures were compared with those of the crystal structure to assess global deformations of the molecule by use of a distance difference map. Since the structural differences between the crystal structure and the equilibrated structure are small (Figure 1), all comparisons are made with respect to the crystal structure, rather than to the equilibrated structure. The distance difference maps compare the α-carbon backbone of the crystal structure (c) and the final structure (f). The value plotted is

$$D_{ij} = |d_{ij}^{c} - d_{ij}^{f}|$$

where i and j indicate α-carbon atoms and the distances between atoms i and j in the crystal structure and in the final structure are indicated by d_{ij}^{c} and d_{ij}^{f}, respectively.

RESULTS

The molecular dynamics simulation of 434(1−63) in a bath of SPC/E water showed the intrinsic stability of this molecule. After 380 ps at 300 K the molecule has remained very close to the starting crystal conformation. In Figure 1 a distance difference map comparing the equilibrated structure to the crystal structure shows how little the conformation of the molecule actually has changed. The last residue on the carboxy terminus changes slightly, and there is a small shift of the first helix relative to the third helix in the molecule.

Separate simulations were performed using the four altered solvent interactions, SPM, SPL, SSM, and SSL, and the structures resulting after 250 ps were compared with the starting crystal structure. In Figure 2a−d the distance difference maps are shown for these four simulations. The simulation SPM (Figure 2a) shows the greatest perturbation with respect to the crystal structure and is also plotted in Figure 2e with a cruder scale to show the extent of the changes. After 250 ps the first and fifth helices have retained their relative positions, but the second, third, and fourth helices are oriented differently relative to the other two. Thus the structure of 434(1−63) is undergoing some major structural rearrangement when exposed to a solvent with stronger water−protein interactions.

In contrast, after 250 ps using the other three altered solvent models the structure of the protein is hardly perturbed at all (Figure 2b−d). In the simulations SPL and SSM a slight perturbation of the loop following the third helix relative to the loop following the first helix occurs. In the simulation SSL, the structure is perturbed somewhat more extensively. Many of the loop regions show structural changes, and the second helix has moved relative to the first one. However, these movements are much smaller in magnitude and extent than those obtained with SPM.

To investigate whether the trends of denaturation observed after 250 ps would propagate, two of these simulations were continued. The SPM simulation was continued for another 250 ps to a total simulation length of 500 ps. The SSL simulation was continued for another 100 ps to a total simulation length of 350 ps. The resulting distance difference maps are shown in Figure 3. In the simulation SPM the trends seen in the first 250 ps (Figure 2a,e) are also observed in the next 250 ps (Figure 3a). The first and fifth helices are separating further from the other three helices, and more movement is observed in the loop regions between the three central helices. Figure 4 compares the crystal structure with the resulting structure after 500 ps in two orientations which are rotated 90° relative to each other. The helices of the structure have thus far remained intact; however, as the distance difference map implies, they have separated from each other. The region of residues 53−60, which is experimentally observed to form a nonrandom structure in 7 M urea, also remains intact in this simulation. Thus during the whole simulation under the SPM solvent conditions the protein is unfolding in a manner which is

Table 2: Intraprotein Hydrogen Bonds Which Occur More than 20% of the Time Averaged over 100 ps[a]

	donor−acceptor	D	H	A	standard	SPM	SPM500	SPL	SSL	SSM	heat
	1 Ser−60 Leu	N	H1	O						20	
	1 Ser−61 Asn	N	H3	O							24
	2 Ile−59 Leu	N	H	O				42			
	2 Ile−60 Leu	N	H	O				26			
	3 Ser−39 Thr	OG	HG	O							32
	4 Ser−1 Ser	N	H	O			51	37			
	4 Ser−63 Thr	OG	HG	O2					83		
	4 Ser−63 Thr	OG	HG	O1					44		
	5 Arg−62 Gly	NE	HE	O							21
	5 Arg−62 Gly	NH2	HH22	O							28
	5 Arg−63 Thr	NE	HE	O1					77		
	5 Arg−58 Trp	NH1	HH12	O				67		32	55
	5 Arg−63 Thr	NH2	HH22	OG1					80		
	5 Arg−63 Thr	NH1	HH11	O2						38	
XN	5 Arg−1 Ser	N	H	O	61	52	51			51	44
XN	5 Arg−59 Leu	NH1	HH12	O	60	84	80		38		
	5 Arg−61 Asn	NH2	HH21	O			25				
XN	6 Val−2 Ile	N	H	O	88	97	93	95	91	98	93
XN	7 Lys−3 Ser	N	H	O	88	79	93	97	89	98	
Xn	7 Lys−35 Glu	NZ	HZ1	OE2					45	42	68
	7 Lys−35 Glu	NZ	HZ2	O					29		
Xn	7 Lys−35 Glu	NZ	HZ2	OE2					28		
XN	8 Ser−4 Ser	N	H	O	98	33	96	96	93	99	90
XN	9 Lys−5 Arg	N	H	O	94	98	38	76	56	88	92
Xn	9 Lys−12 Gln	NZ	HZ2	OE1				55			
	9 Lys−52 Leu	NZ	HZ1	O				34		24	29
XN	10 Arg−6 Val	N	H	O	96	93	87	97	55	97	97
	10 Arg−14 Gly	NH2	HH22	O							32
	10 Arg−17 Gln	NE	HE	OE1	38						24
Xn	10 Arg−15 Leu	NH1	HH12	O	87		55	81		81	35
X	10 Arg−35 Glu	NE	HE	OE2				43			
XN	10 Arg−35 Glu	NH2	HH22	OE2				79		29	
XN	11 Ile−7 Lys	N	H	O	89	93	54	96	90	95	90
XN	12 Gln−8 Ser	N	H	O	97	92		97	98	94	92
XN	13 Leu−9 Lys	N	H	O	97	89		69	98	83	94
	13 Leu−10 Arg	N	H	O					23		
	14 Gly−9 Lys	N	H	O		21	90				
N	14 Gly−10 Arg	N	H	O	21	32		45	22	72	35
Xn	14 Gly−11 Ile	N	H	O	63			40	54		44
XN	15 Leu−10 Arg	N	H	O	77	49			85		
	15 Leu−13 Leu	N	H	O							34
XN	16 Asn−19 Glu	N	H	OE2	52				37		43
	16 Asn−19 Glu	N	H	OE1	37			71	39	72	44
	16 Asn−19 Glu	ND2	HD22	OE2							21
	17 Gln−17 Gln	N	H	OE1							52
	17 Gln−32 Glu	NE2	HE22	OE2	90			95		95	
	17 Gln−31 Ile	NE2	HE21	O	61			38		28	
	17 Gln−34 Leu	NE2	HE21	O			54				
XN	17 Gln−35 Glu	NE2	HE21	OE2					29		
XN	19 Glu−16 Asn	N	H	OD1	69	83	87	70	96	92	
	19 Glu−19 Glu	N	H	OE1							21
	19 Glu−19 Glu	N	H	OE2							27
XN	20 Leu−16 Asn	N	H	O	97	98	94	98	98	100	91
XN	21 Ala−17 Gln	N	H	O	86	96	91	99	96	97	96
XN	22 Gln−18 Ala	N	H	O	95	94	96	97	95	97	79
XN	23 Lys−19 Glu	N	H	O	97	82	68	97	82	93	62
	23 Lys−19 Glu	NZ	HZ2	OE1				45		22	
	23 Lys−19 Glu	NZ	HZ3	OE1				28			
XN	24 Val−20 Leu	N	H	O	92	74	77	94	35	99	53
	25 Gly−21 Ala	N	H	O	44				53		
	25 Gly−22 Gln	N	H	O	29	45		69	33	58	
XN	26 Thr−21 Ala	N	H	O	86	83	55	91	44	96	42
	26 Thr−24 Val	OG1	HG1	O			91				
	26 Thr−47 Glu	N	H	OE1					22		
	28 Gln−32 Glu	NE2	HE21	OE1							28
	28 Gln−32 Glu	Ne2	HE21	OE2	75			64	20	25	61
	29 Gln−28 Gln	NE2	HE22	OE1							58
	29 Gln−32 Glu	NE2	HE21	OE1							29
	29 Gln−33 Gln	NE2	HE22	OE1						39	
	30 Ser−27 Thr	N	H	OG1	29	26		31	33	65	29
N	30 Ser−27 Thr	N	H	O	25			23	21		30
	30 Ser−26 Thr	OG	HG	OG1				80	24	75	
	31 Ile−27 Thr	N	H	O	23	74		24	45	54	
	31 Ile−28 Gln	N	H	O	20						

Table 2 (Continued)

	donor−acceptor	D	H	A	standard	SPM	SPM500	SPL	SSL	SSM	heat
XN	32 Glu−28 Gln	N	H	O	94	66	84	98	98	99	92
XN	33 Gln−29 Gln	N	H	O	98			89	95	96	91
	33 Gln−29 Gln	NE2	HE22	O				36			
	33 Gln−29 Gln	NE2	HE22	OE1				21			
	33 Gln−30 Ser	N	H	O		41					
XN	34 Leu−30 Ser	N	H	O	73		75	75	46	30	
	34 Leu−31 Ile	N	H	O						38	25
XN	35 Glu−31 Ile	N	H	O	96	76	56	97	83	82	91
	35 Glu−32 Glu	N	H	O			27				
N	36 Asn−32 Glu	N	H	O	94	54		90	73	79	94
	36 Asn−35 Glu	ND2	HD22	OE1							20
	37 Gly−33 Gln	N	H	O		40					
N	37 Gly−34 Leu	N	H	O	58	38	70		64	29	68
XN	38 Lys−33 Gln	N	H	O	80	83	72	89	82	76	60
	38 Lys−36 Asn	NZ	HZ1	O				41			
	39 Thr−33 Gln	N	H	O	32			52		67	51
	39 Thr−33 Gln	OG1	HG1	O						20	
	43 Arg−47 Glu	NH1	HH11	OE1				59			
	43 Arg−47 Glu	NH2	HH21	OE1				56			
	43 Arg−47 Glu	NH2	HH21	OE2				37			
	44 Phe−42 Pro	N	H	O		39					
	45 Leu−43 Arg	N	H	O	71	36	75	65	51	81	70
	47 Glu−47 Glu	N	H	OE1							52
	47 Glu−47 Glu	N	H	OE2				95		96	30
XN	48 Leu−44 Phe	N	H	O	98	98	95	98	99	98	93
XN	49 Ala−45 Leu	N	H	O	97	97	98	96	93	58	93
XN	50 Ser−46 Pro	N	H	O	94	88	88	91	97	96	91
XN	51 Ala−47 Glu	N	H	O	87	91	86	87	93	91	93
XN	52 Leu−48 Leu	N	H	O	88	98	95	97	90	91	89
N	53 Gly−49 Ala	N	H	O		68	59	24			28
X	53 Gly−50 Ser	N	H	O	71			50	63	62	48
XN	54 Val−49 Ala	N	H	O	93			91	86	87	86
	54 Val−52 Leu	N	H	O		52	34				
	57 Asp−55 Ser	N	H	OG							27
Xn	58 Trp−55 Ser	N	H	OG	26	28	56	66	65	63	21
N	59 Leu−55 Ser	N	H	O	93	96	96	84	94	65	30
XN	60 Leu−56 Val	N	H	O	88	85	67	93	86	85	81
XN	61 Asn−57 Asp	N	H	O	94	22		78	92	60	82
	61 Asn−57 Asp	ND2	HD22	OD2	38			78		82	
	61 Asn−57 Asp	ND2	HD22	OD1	28					32	
	62 Gly−57 Asp	N	H	O						48	
	63 Thr−63 Thr	OG1	HG1	O1							23

[a] The first column denotes whether a hydrogen bond is observed in the X-ray (X) (Mondragon et al., 1989) or NMR (N) structure as noted in Neri et al. (1992a). A lower case n means it is only seen in less than 5 of the 20 NMR conformers used to represent the solution structure. For the definition of the other symbols, see caption for Table 1.

structurally consistent with what has been observed experimentally.

In contrast to the results from the continuation of the SPM simulation, the structure of 434(1−63) under SSL solvent conditions (Figure 3b) actually returned to being more native-like after another 100 ps of dynamics. Thus the structural changes seen after 250 ps (Figure 2d) were temporary perturbations and do not seem to represent denaturation of the molecule.

Increasing the temperature is an alternative technique to denature a protein. Figure 5 shows the distance difference map resulting from a 500 ps MD simulation of the standard system at the elevated temperature of 360 K. Some movement of the helices is seen, yet they are much smaller in magnitude than those observed for the same length simulation under the SPM solvent condition. For the most part structural changes are restricted to loops of the protein and are less than 3 Å in magnitude.

The distance difference maps give only a global picture of the actual denaturation of the molecule. They do not yield the detailed information on the behavior of the solvent. Since during the molecular dynamics simulations the configurations of all atoms in the system were saved every 0.2 ps, an analysis of intermolecular hydrogen-bonding interactions between the water molecules and the protein and the intramolecular hydrogen bonding within the protein is possible. The interactions are divided into three types: hydrogen bonds of water with the polar peptide backbone atoms, hydrogen bonds of water to side-chain atoms, and intramolecular hydrogen bonds within the protein. For every simulation the percentage of time a particular hydrogen bond is present in a 100 ps period is calculated. The hydrogen bonding was analyzed for the time period 150−250 ps for the solvent simulations with the four altered interactions. In addition, the simulation using the SPM solvent condition was analyzed during the period from 400 to 500 ps. The equilibration simulation was analyzed from 340 to 440 ps and the simulation at 360 K from 400 to 500 ps. Hydrogen bonds between protein and water are given in terms of percentile change between the altered solvent environment and the normal SPC/E solvent. Since an oxygen atom can accept more than one hydrogen bond simultaneously, some atoms show more than 100% hydrogen bonding. In Figure 6a−d the percentile change of water hydrogen bonds to the

protein backbone between the altered solvent and the normal SPC/E solvent is plotted for the four simulations. Table 1 gives the changes in hydrogen bonding of the side chains to water.

The plot for the SPM simulation (Figure 6a) shows, not unexpectedly, a higher percentage of hydrogen bonds between water molecules and the polar backbone atoms (solid bars). This trend is continued as the simulation proceeds. Table 1 shows that on average the percentile of hydrogen bonds between side chains and water is also increased with this altered interaction. The increase of hydrogen bonding between water and protein correlates with the denaturation of the protein. The region of residues 53−60 in the structure, which is experimentally observed to form a nonrandom structure in 7 M urea (Neri et al., 1992b), a hydrophobic cluster, remained intact for the duration of the SPM simulation. A comparison with the list of NOE-derived upper bounds to atom−atom distances from Neri et al. (1992b) shows that 9 of the 28 distances are violated. However, all but one of the bounds that are violated are also violated in the crystal structure that was used as the starting point for the simulations.

The changes in the atomic interactions clearly influence the average hydrogen bonding of the protein with water in a consistent way (Figure 6 and Table 1). In the SPM solvent, the solvent−protein interaction is strengthened, and the percentage of time a hydrogen bond is formed between water and protein is increased. In the SPL solvent, the solvent−protein interaction is weakened, and the percentage of time a hydrogen bond is formed between water and the protein is decreased. In the SSM solvent, the solvent−solvent interaction is strengthened; thus the water prefers to interact with itself rather than with the protein, and the percentage of time a hydrogen bond is formed between water and protein is decreased. In the SSL solvent, the solvent−solvent interaction is weakened, and thus the percentage of time a hydrogen bond is formed between water and protein is increased. However, the fact that the water prefers to be bound to the protein rather than to itself does not cause the protein to begin to unfold.

In Figure 6e the difference in hydrogen bonding of water to the backbone between the simulation at 360 K and that at 300 K is shown. The elevation of the temperature mainly decreases the percentage of time a water molecule binds to a particular site and does not induce the protein to begin to unfold.

Intramolecular hydrogen bonds stabilize the intact protein fold; thus monitoring them during a simulation is a means to assess whether the protein remains folded or not. In Table 2 intramolecular hydrogen bonds that occur more than 20% of the time are shown and compared with the hydrogen bonds observed in the X-ray crystal structure and the NMR solution structures of the protein. The increase of the solvent-protein interaction (SPM), not unexpectedly, decreases the number of internal hydrogen bonds, since water has replaced many of the internal interactions and the protein is unfolding. The decrease of the protein−solvent interaction (SPL) increases the number and percentage of the internal hydrogen bonds formed in the protein. Strengthening the solvent−solvent interaction (SSM) also slightly increases the internal hydrogen bonding within the protein; if a hydrogen-bonding partner is not being satisfied by interaction with water, then it will tend to find a protein partner, as is generally observed in vacuum simulations. In the simulation with the weaker solvent−solvent interaction (SSL) the native set of hydrogen bonds is the best maintained of all the altered water states. Although water is binding more tightly to the protein in this simulation than in the equilibration simulation using normal water, the water is less likely to bind to itself than it can under standard conditions and is unable to disrupt the protein−protein hydrogen bonds.

DISCUSSION

By altering solvent−protein or solvent−solvent interactions, we aim at mimicking the effects of addition of denaturant to a solution containing protein. Increasing the solvent−protein Coulombic interaction causes denaturation of the 434 repressor DNA binding domain, which is in contrast to decreasing this interaction or altering the corresponding solvent−solvent interaction. The enhanced solvent−protein interaction leads to an increase of solvent−protein hydrogen bonding, which replaces protein−protein hydrogen bonding. This result can be interpreted in two ways:

(1) The altered solvent molecules assume the role of the denaturant molecules. In this model a denaturant exerts its denaturing effect by a direct strong interaction with the protein. The denaturant penetrates the protein, thus breaking the protein−protein hydrogen bonds and unfolding the protein.

(2) The altered solvent molecules are acting as water molecules under the influence of an external agent (a denaturant) which is driving them out of the bulk solvent and into the protein. As more water molecules penetrate into the protein, the protein−protein hydrogen bonds are broken and the protein unfolds.

Our simulations alone, however, are not enough to distinguish whether the initial steps of a protein unfolding are caused by water or denaturant molecules, since there is no explicit denaturant in the simulation. In addition, since the denaturing effect is caused by modifying the Coulombic interaction, these simulations also cannot test whether urea is able to keep a protein soluble by interacting with hydrophobic (electrostatically neutral) side chains. From the simulations only an increase in the solvent−protein Coulombic interaction causes the protein to begin unfolding. This implies that the effect of the denaturant to cause a protein to unfold is to disrupt the subtle balance between the protein−protein interaction and the solvent−protein interaction. Altering the solvent−solvent interaction does not disrupt this balance.

REFERENCES

Berendsen, H. J. C., Postma, J. P. M., van Gunsteren, W. F., DiNola, A., & Haak, J. R. (1984) *J. Chem. Phys. 81*, 3684−3690.

Berendsen, H. J. C., Grigera, J. R., & Straatsma, T. P. (1987) *J. Phys. Chem. 91*, 6269−6271.

Caflisch, A., & Karplus, M. (1994) *Proc. Natl. Acad. Sci. U.S.A. 91*, 1746−1750.

Daggett, V., & Levitt, M. (1992) *Proc. Natl. Acad. Sci. U.S.A. 89*, 5142−5146.

Daggett, V., & Levitt, M. (1993) *J. Mol. Biol. 232*, 600−619.

Dötsch, V., Wider, G., Siegal, G., & Wüthrich, K. (1995a) *FEBS Lett. 366*, 6−10.

Dötsch, V., Wider, G., Siegal, G., & Wüthrich, K. (1995b) *FEBS Lett.* (submitted for publication).

Duffy, E. M., Kowalczyk, P. J., & Jorgensen, W. L. (1993) *J. Am. Chem. Soc. 115*, 9271−9275.

Hao, M. H., Pincus, M. R., Rackovsky, S., & Scheraga, H. A. (1993) *Biochemistry 32*, 9614−9631.
Hünenberger, P. H., Mark, A. E., & van Gunsteren, W. F. (1995) *Proteins 21*, 196−213.
Kraulis, P. J. (1991) *J. Appl. Crystallogr. 24*, 946−950.
Lapanje, S., Lunder, M., Vlachy, V., & Skerjanc, J. (1976) *Biochim. Biophys. Acta 433*, 37636−37640.
Liepinsh, E., & Otting, G. (1994) *J. Am. Chem. Soc. 116*, 9670−9674.
Mark, A. E., & van Gunsteren, W. F. (1992) *Biochemistry 31*, 7745−7748.
Mark, A. E., van Helden, S. P., Smith, P. E., Janssen, L. H. M., & van Gunsteren, W. F. (1994) *J. Am. Chem. Soc. 116*, 6293−6302.
Mondragon, A., Subbiah, S., Almo, S. C., Drottar, M., & Harrison, S. C. (1989) *J. Mol. Biol. 205*, 189−200.
Neri, D., Billeter, M., & Wüthrich, K. (1992a) *J. Mol. Biol. 223*, 743−767.
Neri, D., Billeter, M., Wider, G., & Wüthrich, K. (1992b) *Science 257*, 1559−1563.
Neri, D., Wider, G., & Wüthrich, K. (1992c) *FEBS Lett. 303*, 129−135.
Neri, D., Wider, G., & Wüthrich, K. (1992d) *Proc. Natl. Acad. Sci. U.S.A. 89*, 4397−4401.
Pace, C. N. (1986) *Methods Enzymol. 131*, 266−280.
Pace, C. N., Laurents, D. V., & Erickson, R. E. (1992) *Biochemistry 31*, 2728−2734.
Ryckaert, J.-P., Ciccotti, G., & Berendsen, H. J. C. (1977) *J. Comput. Phys. 23*, 327−341.
Schiffer, C. A., & van Gunsteren, W. F. (1995) *Proteins* (submitted for publication).
Shimon, L. J. W., & Harrison, S. C. (1993) *J. Mol. Biol. 232*, 826−838.
Tirado-Rives, J., & Jorgensen, W. L. (1993) *Biochemistry 32*, 4175−4184.
van Gunsteren, W. F., & Berendsen, H. J. C. (1987) *Groningen Molecular Simulation (GROMOS) Library Manual*, Biomos, Groningen, The Netherlands.

BI951153F